Nanotechnological Applications of Zinc Oxide Nanoparticles and its correlation with Structural and Magnetic Properties

Dr. Ritu
Department of chemistry, Chhotu Ram Arya Collage, Sonepat-131001 (Haryana)

Received: July 08, 2018 Accepted: August 12, 2018

ABSTRACT *Nanosized zinc oxide was synthesised using a simple and effective method of precipitation "from zinc nitrate and liquid ammonia with a 5-hour step of calcination at high temperature at 5000C. XRD (X-ray diffraction), TGA / DTA (Thermal Gravimetry Analysis and Differential Thermal Analysis), Scanning Electron Microscopy (SEM) / Transmission Electron Microscopy (TEM) and magnetic measuring techniques were used to classify the nanosized ZnO." Studies on XRD have shown "that zinc oxide was formed as ZnO and that it has a crystal structure of hexagonal wartzite. The TEM calculated the particle size of the synthesised zinc oxide. TEM images showed that the zinc oxide particle size ranged from 21-40 nm, which is in good alignment with the nanomaterial size theoretically expected. Compared with the known methods for nanomaterial synthesis this method is cheaper, easier and more efficient. Excellent consensus exists between the experimental and theoretical findings.*

Keywords: *Nanomaterials, Zinc Oxide, Transmission Electron Microscopy (TEM), XRD analysis."*

1. INTRODUCTION

Metal oxides have received a lot of popularity in recent years because of their capacity to survive harsh process environments. For humans and animals, metal oxides like NiO and ZnO are of special concern, as they are considered healthy materials. The use of zinc oxide was considered a viable option for environmental protection. Nanotechnology has recently emerged as a leading powerhouse in science and technology. Nanotechnology is expected to be the second most recent technological revolution in the world. Global attention across disciplines has been attracted to new properties. ZnO nanoparticles demonstrate stable luminous photoluminescence in colloidal dispersion [1].

ZnO is a flexible material used for semiconductors [2]. Zno has a bandgap energy of 3.37 eV and, at room temperature, has a very high excitation binding energy (60 meV). It is rotzite of the semiconductor type [3]. Due to its need for thermal stability, the versatility of modeling different nanostructures, the commercial demand for optoelectronic devices, ZnO has recently sparked interest. Several nanostructures [4-6] can form ZnO. ZnO is commonly used in surface acoustic wave devices [7], field emissions [8], gas sensors [9], ceramics [10], solar cells [11], biosensors [12], varistors [14], electrodeposition [16], antimicrobial fabrics [17], catalysis, biotechnologies for environmental safety, piezoelectric behavior [18-21] and ultraviolet nanolayers [22].

2. EXPERIMENTAL PART

2.1 Chemicals

"All chemicals used in the experiment are of analytic reagent grade. Zinc nitrate i.e. Zn $(NO_3)_2$ was purchased from MERC, India. Liquid ammonia was also purchased from MERCK, India. Deionized water was used throughout the experiment".

2.2 Synthesis of ZnO

500 ml of 0.5 M solution of Zn (NO3) 2 were taken and aqueous ammonia was added drop by drop under continuous stirring until a pH 10 solution was reached. The precipitate thus obtained was filtered on a Buckner funnel and washed several times with distilled water. The precipitate was dried for 24 hours in an oven at 700 ° C and calcined for 5 hours in a muffle oven at 5000 ° C. The material obtained was ground and sewn through a 100 mesh screen.

2.3 Equipments

2.3 Equipment Used :

Utilizing power X-ray diffraction patterns, analysis or structural learning for synthesized oxides was reported utilizing power X-ray diffraction patterns. Rigaku rotating anode Ru-H3R X-ray diffractometer as well as Brucker D8 high resolution diffraction ate and PAN analytical Experts Pro diffractometer employing CuKα (λ=1.5404A^0) radiation. The crystalline size of Zinc ferrite was calculated using Scherrer equation .

$t = K\lambda / B \cos\theta$

If t is the average size of the crystallites of the process under examination, K is the Scherrer constant (0.89), λ is the wavelength of the X-ray beam used, B is the half-complete diffraction (in radians) limit (FWHM) and??is the Bragg angle. Transmission electron micrograph (TEM) was recorded on the Hitachi H7500. The samples were dispersed in ethanol and ultrasonically treated to disperse individual particles on a gold grid. Using a model 155 vibrating sample magnetometer, the magnetic properties of the solid at room temperature were calculated. Using the electron microscope Quanta 200 FEG (FEI Holland), the surface morphology of the nickel oxide prepared by the precipitation method was studied.

2.3.4 Calibration of pH meter.

"We calibrated the pH meter using buffer solution of pH4, pH7 and pH9".

3.RESULTS AND DISCUSSION

X-Ray Studies:

The properties or efficacy of both the different devices were, as has been understood, highly due to the surface characteristics. That synthesised zinc oxide is seen with radiological diffraction in fig. Uh. (one). (A). (One). Pure zinc oxide X-ray diffraction pattern indicated zinc oxide and in shape of a hexagonal verzite structure of ZnO Fig. A. (A). (one). In X-ray diffraction several influential peaks are called as well as the resulting "d-values (2.8179, 2.6049, 2.4786 .....) are compared with JCPDS file standards no. 80-0075 (Table No. 1). X-ray diffraction shows the pure ZnO metal oxide has monocrystalline ZnO but has a hexagonal form of wartzite". A high degree of orientation is shown by X-ray diffraction. That form was shown to be anisotropic, and it can be interpreted in medium crystallites to cones, however in fact these become right prisms with such an unusual hexagon cross-section. In addition, the Scherrer equation calculated the size of both the crystals but it was observed to encourage TEM tests. The X-ray diffraction evidence reveals the ZnO nanoparticles' hexagonal unitary cell structure. It was discovered that the actual nanoparticles have been between 21 and 40 nm in height. The experimental and numerical findings are in outstanding agreement.

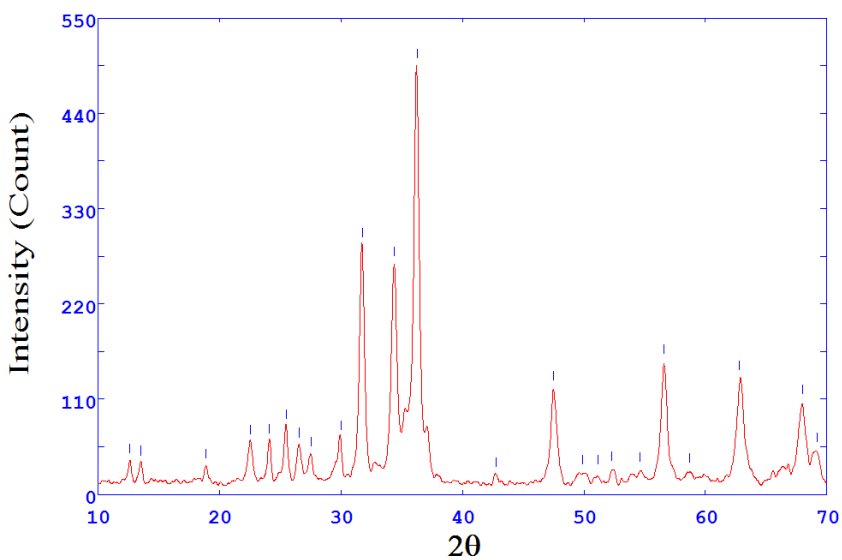

Fig. 1: X-ray diffraction patterns of Calcined sample after calcinations

TABLE-1:- X-RAY DIFFRACTION DATA OF ZINC OXIDE

S.No.	d=λ/2Sinθ (Observed)	d=λ/2Sinθ (Reported)	I/I_0x100% Observed	I/I_0x100% Reported
1	2.8179	2.8179	57.86	57.86
2	2.6049	2.6048	44.24	44.25
3	2.4786	2.4785	100	99.99
4	1.9128	1.9128	22.92	22.92
5	1.6269	1.6269	32.43	32.45

6	1.4784	1.4785	27.62	27.64
7	1.4089	1.4087	4.40	4.39
8	1.3789	1.3789	24.32	24.30
9	1.3601	1.3601	11.41	11.41
10	1.3024	1.3025	1.90	1.91
11	1.2393	1.2392	3.80	3.81
12	1.1822	1.1822	1.90	1.90

Thermal Analysis:

Thermal analysis comprises a collection of techniques where a substance 's physical property are calculated in such a thermo-regulated environment as both a function of time and temperature. "Includes thermo gravity (TG), differential thermal analysis (DTA) and derived thermo gravimetry (DTG)". The thermo gravimetric experiments were conducted in a temperature range of 10-10000 ° C in an N2 atmosphere. The figure shows the TGA / DTA oxide curves. Table (2) summarizes the total gross Zinc oxide weight loss as well as its associated temperature. Those findings revealed some weight loss or oxide decay, dehydration or physical transformation mostly on synthesized oxides. They find the zinc oxides exhibit a steady loss of weight below 959,880 ° C. Even in the DTA curve, exothermic and endothermic peaks indicate phase transition, the achievement of solid state in "any chemical reaction that occurs during heat treatment. From the TGA curve we observe a constant weight loss above 959.880 ° C [Fig. 2]."

TABLE: 2: OBSERVATIONS OF WEIGHT LOSS FOR ZINC OXIDE AT CORRESPONDING TEMPERATURE RANGE

Sr.No.	Maximum % loss in weight	Temperature range ^{0}C
1	16.817%	35.03-425^{0}C
2	13.212%	691.58-959.88^{0}C

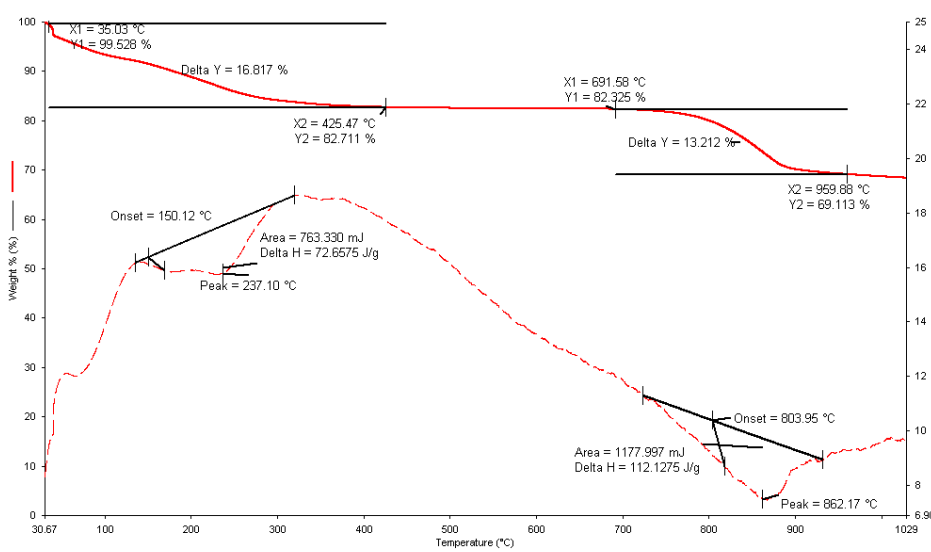

Fig: 2: TGA-DTA graph of Zinc Oxide.

Magnetic Measurements:

Zinc oxide at room temperature is amphoteric and semiconductor oxide Excellent piezoelectric properties. Ferromagnetic activity at room temperature can be induced in the ZnO nano particles excluding doping of magnetic contaminants, and merely through allowing their electron structure to change ferro magnetically, (Figure 3).

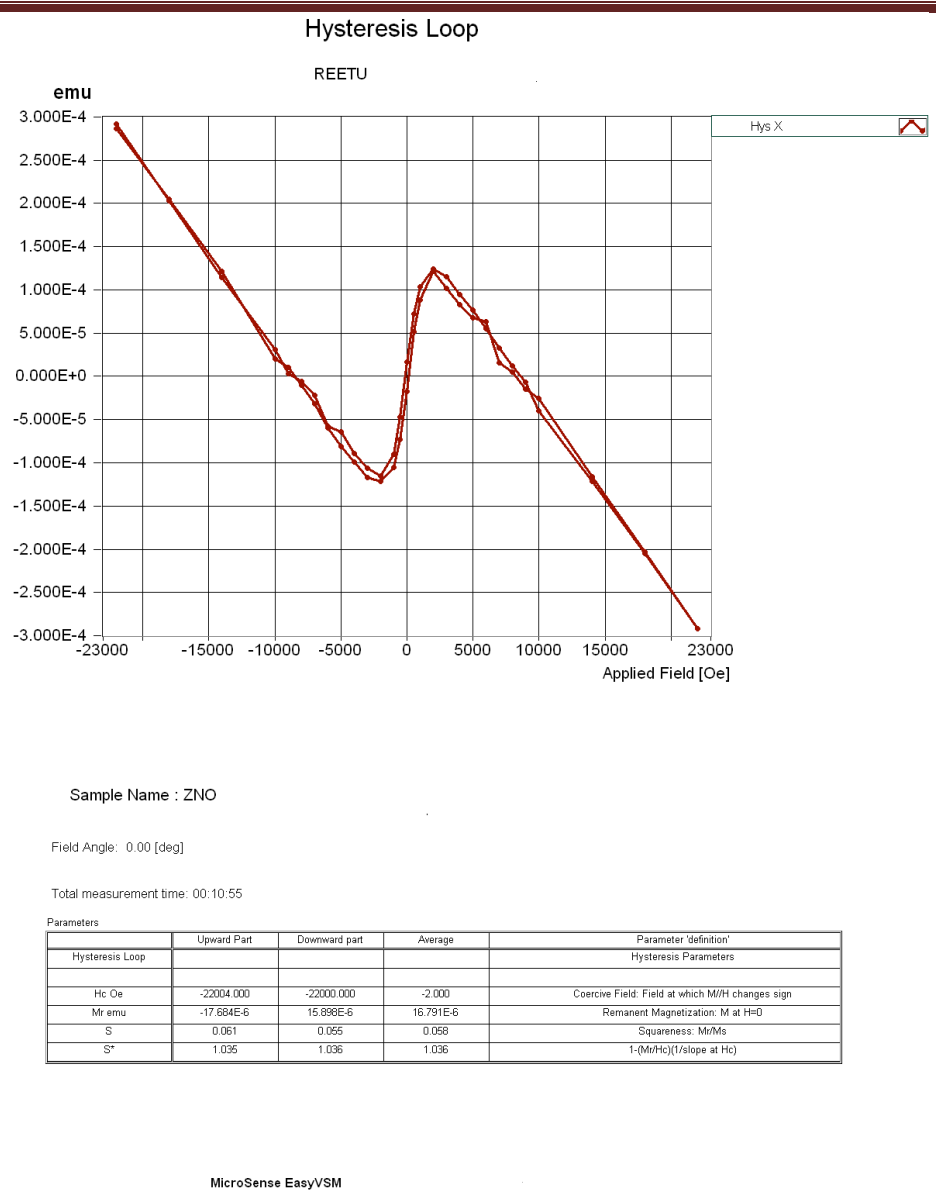

	Upward Part	Downward part	Average	Parameter 'definition'
Hysteresis Loop				Hysteresis Parameters
Hc Oe	-22004.000	-22000.000	-2.000	Coercive Field: Field at which M//H changes sign
Mr emu	-17.684E-6	15.898E-6	16.791E-6	Remanent Magnetization: M at H=0
S	0.061	0.055	0.058	Squareness: Mr/Ms
S*	1.035	1.036	1.036	1-(Mr/Hc)(1/slope at Hc)

Fig.3 Manetic measurements of synthesized ZnO

SEM and TEM Studies :

Sample morphology was investigated with the assistance of SEM and TEM. Sections [a, b , c] fig. 4 Displays standard sample SEM images. Scanning electron microscopy reveals Zinc Oxide's hexagonal form. (4). (4). SEM photos display a significant quantity of bunches-like flowers. Each bunch gathers tightly packed nanometer scale rods. Parts[a] and[b] of fig.5 display sample TEM images. Part[b] observes the nanostructure-like flora. During TEM preparation, flowers like nanostructures were not killed. This suggests that blooming like nanostructures is not due to aggregation.

"TEM is evidence for formation of hexagonal ZnO nanoparticles (Wurtzite structural type fig.5) .TEM studies show that the ZnO nanoparticle is hexagonal and size of the obtained nanoparticles is in the range 21-40 nm. Table No.(3)".

Conclusion:

In conclusion, a general and simple approach was produced for the preparation of nanoscale zinc oxide by aqueous precipitation from commercially available reagents. The experimental and theoretical results coincide excellently. In zinc oxide nanoparticles there is an excellent approach Along with aqueous precipitation process, from both the viewpoint of quicker , cheaper and simpler storage, but from the determination of both the fundamental properties. That findings indicate nano-sized nanoparticles of zinc

oxide with such a hexagonal crystal structure of quartzite. TEM Studies reveal the particles are 21 to 40 nm average in size. Studies by SEM demonstrate that there is a ZnO hexagonal structure. Ferromagnetic attributes were demonstrated in magnetic experiments. The whole technique is beneficial over conventional zinc oxide synthesis approaches on a nanoscale. The proposed approach is however very exciting, and also has substantial implementations.

TABLE-3:- PRACTICAL SIZE OF SYNTHESIZED ZINC OXIDE AT DIFFERENT SCALES

S.No.	Scale (20nm)	Scale (100nm)
1	39	38
2	36	37
3	35	35
4	21	21
5	37	37
6	38	38
7	37	36
8	26	25
9	40	39
10	40	40
Range	21nm to 40nm	21nm to 40nm

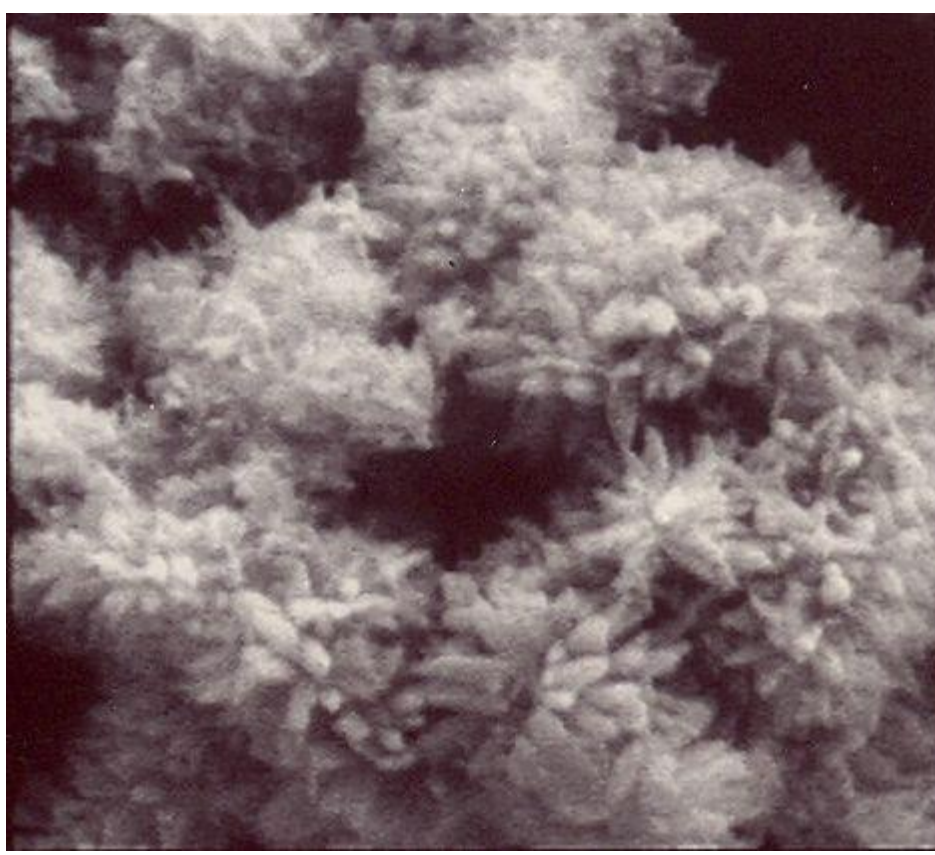

Fig.4(a) SEM Micrographs of Zinc oxide

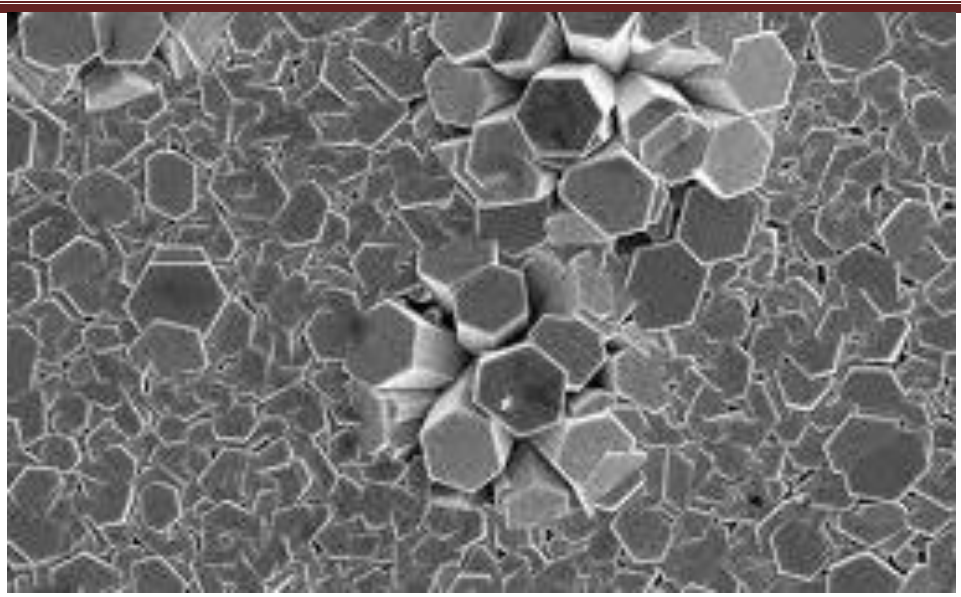

Fig.4(b) SEM Micrographs of Zinc oxide

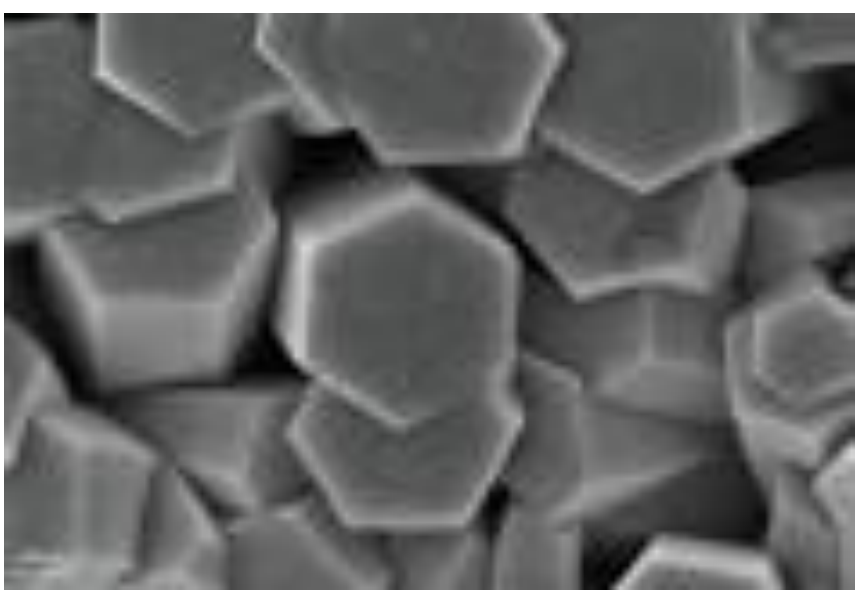

Fig.4(c) SEM Micrographs of Zinc oxide

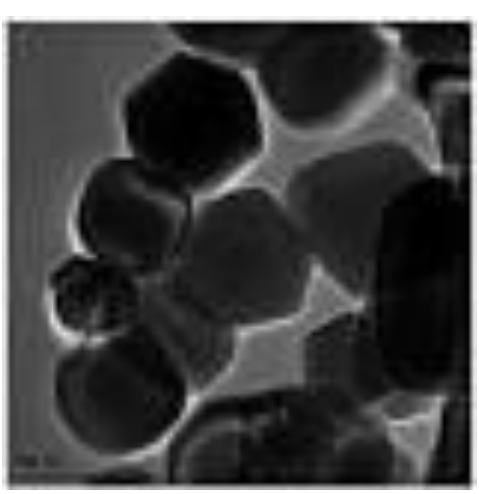

Fig. 5(a) TEM micrographs of Zinc Oxide under high magnification (Scale bar is 20 nanometer

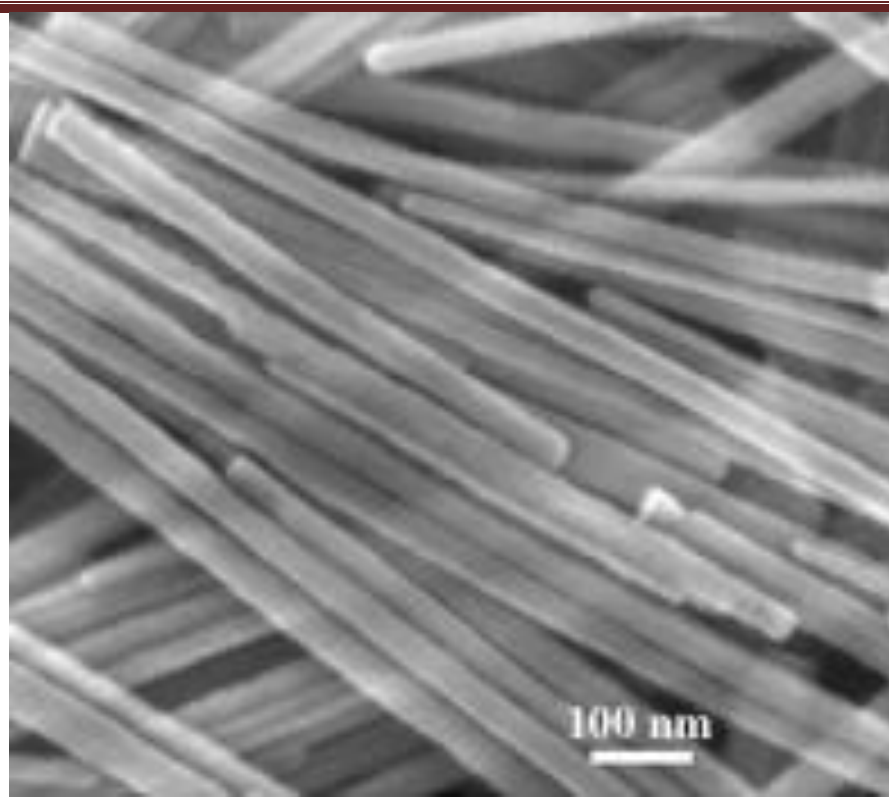

Fig. 5(b): TEM micrographs of Zinc Oxide under low magnification (Scale bar is 100nm)

REFERENCES

1. H.M Xiong ,D.G.Shchukin , H.Mohwald, Y.Xu andY.Y.Xia, Angewandte Chemie International Edition, 48 , **15** (2009) 2727-2731
2. D.C.Look , Mater.Sci.Eng.B **80** (2001) 383
3. C.M. Lieber , Solid State Communication ,**66** (1998) 5309
4. Y.Zhang , K.Suenaga, C. Collies, S.Iijima , Science **281** (1998) 973
5. L.Vayssieres, K.Kies ,A.Hagfeldt, S.E.Lindquist, Chem. Mater, **13** (2001) 4395
6. Z.W.Pan , Z.R.Dai, Z.L.Wang, Science **292** (2001) 1947
7. W.C.Schin, M.S. Wu, J.Cryst. Growth **137** (1994) 319
8. C.X.Xu, X.W.Sun , Appl. Phys. Lett. **83** (2003) 3806
9. R.Paneva, D.Gotchev,Sens.Actuat.A :Phys.**72** (1999) 79
10. L.Gao,Q.Li, W.L.Luan, J.Am. Ceram.Soc. **85** (2002) 1016
11. N.F.Cooray, K.Kushiya, A.Fujimaki, D.Okumura,M.Sato, M.Ooshita, O.Yamase,Jpn.J.Appl. Phys. **38** (1999) 6213
12. P.X.Gao, Y.Ding ,W.Mai, W.L.Huges, C.S.Lao, Z.L.Wang, Science **309** (2005) 1700
13. E.Topoglidis, A.E.G.Cass, B.Oregan, J.R.Durrant, J.Electoanal. Chem. **517** (2001) 20
14. N.T.Hung, N.D.Quang, S.Bernick, J.Mater. Res. **16** (2001) 2817
15. J.A.Rodriguez, T.Jirsak, J.Dvorak,S.Sambasivan, D.J.Fisher, J.Phys. Chem. B **104** (2000) 319
16. A.B.Moghaddam, T.Nazari,J.Badraghi and M.Kazemzad ,Int.J. Electochem. Sci. , **4** (2009) 247-257
17. R.Rajendran, C.Balakumar, H.A.M. Ahammed , S.Jayakumar, K.Vaideki and E.M.Rajesh, Int. J. of Engineering Science and Technology ,2, **1** (2010) 202-208
18. Z.L. Wang and J.Song ,"Piezoelectric naogenerators based on zinc oxide nanowire arrays," Science ,312, **5771** (2006) 242-246
19. X.Wang ,J.Song,J.Liu and L.W.Zhong, "Direct-Current nanogenerator driven by ultrasonic waves," Science , 316, **5821** (2007) 102-105
20. C.Chang, V.H.Tran ,J.Wang, Y.K.Fuh and L.Lin ,"Direct write piezoelectric polymeric nanogenerator with high energy conversion efficiency," Nanoletters ,10, **2** (2010) 726-731
21. S.Xu, Y.Quin, C.Xu,Y.Wei,R.Yang and Z.L. Wang ,"Self powered nanowire devices" Nature Nanotechnology,5, **5** (2010) 366-373
22. H.M.Huang,S.Mao, H.Fecik, H.Yan, Y.Wu,H.Kind,E.Weber,R.Russo, P.D.Yang, Science **292** (2001) 1897